

# RE-ENTRY VEHICLE DESIGN BY MULTIDISCIPLINARY OPTIMISATION IN ASTOS

Irene Huertas<sup>(1)</sup>, Christian Möllmann<sup>(1)</sup>, Sven Weikert<sup>(2)</sup>, Alvaro Martinez Barrio<sup>(2)</sup>

<sup>(1)</sup> Astos Solutions GmbH, Meitnerstr. 10, 70563 Stuttgart, Germany, [Irene.Huertas@astos.de](mailto:Irene.Huertas@astos.de)

<sup>(1)</sup> Astos Solutions GmbH, Meitnerstr. 10, 70563 Stuttgart, Germany, [Christian.Moellmann@astos.de](mailto:Christian.Moellmann@astos.de)

<sup>(1)</sup> Astos Solutions GmbH, Meitnerstr. 10, 70563 Stuttgart, Germany, [Sven.Weikert@astos.de](mailto:Sven.Weikert@astos.de)

<sup>(2)</sup> European Space Agency, Keplerlaan 1, 2200 AG Noordwijk, The Netherlands, [Alvaro.Martinez.Barrio@esa.int](mailto:Alvaro.Martinez.Barrio@esa.int)

## ABSTRACT

During design, re-entry vehicles are optimised to improve their properties, such as lift-to-drag ratio, or overall mass. ASTOS, the AeroSpace Trajectory Optimization Software, now includes a new feature to concurrently optimise the vehicle's shape and TPS sizing, on top of trajectory optimisation, to produce optimal design results.

The usual approach is to optimise the three aspects separately and iterate between optimisations until convergence is achieved. The approach shown here is to use only one optimisation problem so the influence of every optimisable parameter on the cost function (and the constraints) is immediately recognized by the optimiser. This conveys two advantages: 1) using a gradient-based optimiser ensuring superlinear convergence and 2) the user can optimise within all-in-one tool ASTOS providing extensive aerospace specific analysis functionalities.

The vehicle's shape can be optimized starting from predefined parameterised shapes. The disciplines that influence the design of the re-entry vehicle are: aerodynamics, trajectory and thermodynamics.

## 1. CONCURRENT DESIGN OPTIMISATION OF RE-ENTRY VEHICLES

Multidisciplinary optimisation is a field of engineering that concerns itself with the optimisation of a design. This task is achieved by taking into account all the disciplines that are involved in the process, and by regulating those design variables that intertwine the disciplines so as to obtain the best overall design. In this process the influences of these variables are studied and compromises are made. This field has already been in use since the beginning of the aerospace industry. In the last twenty years many engineers and scientists have been trying to automate this process to a certain degree in order to make this optimisation easier, faster and therefore also cheaper.

Aircraft and spacecraft conceptual design is a problem with multiple, loosely coupled disciplines with a large number of global variables. On top of this the disciplines are not independent but are interconnected through a series of design variables that have opposite effects in the disciplinary performance. This means that a large interaction between the disciplines and their experts is required in order to achieve a design that is

acceptable to all disciplines and has a good performance overall.

Each discipline contains parametric relation variables and optimisation variables. Parametric relation variables are those variables within a discipline needed to calculate output (cost functions, constraints and auxiliary variables). Optimisable parameters are those parameters that can be controlled by the optimiser to influence the output values. Furthermore the disciplines expect certain variables from other disciplines as input for their own, and generate output that is in turn used as input by other disciplines. Finally, there are model parameters within each discipline that the user has to set according to the re-entry vehicle type.

The disciplines taken into account in the optimisation of a re-entry vehicle design are:

- Trajectory
- Aerodynamics
- Thermodynamics
- Weights

The software ASTOS currently makes use of the AAO (All-At-Once) method to perform the trajectory optimisation of a re-entry vehicle [1]. The AAO method uses only one optimisation problem and the influence of every optimisable parameter on the cost function (and the constraints) is immediately recognized by the optimiser. This conveys two advantages. First, using a gradient-based optimiser (e.g. Sequential Quadratic Programming, SQP) ensures superlinear convergence in contrast to splitting the problem into several optimisations where no mathematical convergence proof can be given. Secondly, the user can optimise within the all-in-one tool ASTOS providing him with extensive aerospace specific analysis functionalities.

## 2. ASTOS

ASTOS software is a simulation and optimization environment to compute optimal trajectories for a variety of complex multi-phase optimal control problems. It has been developed for the last 20 years and is a reference tool for space trajectory optimisation at ESA/ESTEC. It consists of fast and powerful optimization programs that handle large and highly discretised problems, a user interface with multiple plot capability, and GISMO, an integrated graphical iteration monitor to review the optimization process and plot the

state and control histories at intermediate steps during the optimization.

In ASTOS the trajectory is split into several phases, which allows the definition of intermediate boundary constraints and cost functions as well as of changing discretised states, discretised controls and design.

The discretised multi-phase optimal control problem is transferred into a parameter optimisation problem either by Direct Multiple Shooting or by Direct Collocation. The following transcription methods are provided:

- PROMIS, PaRameterized Optimal Control Using Multiple Shooting
- TROPIC, Trajectory Optimisation by direct Collocation
- CAMTOS, Collocation And Multiple-Shooting Trajectory Optimisation Software
- SOCS, Sparse Optimal Control Software

All transcription methods solve the parameter optimisation problem with sparse Non-Linear Programming (NLP) solvers like SNOPT, WORHP, ipfilter, SPRNLP and others. More than 100.000 optimisable parameters can be handled by some of the solvers. Also dense NLP solvers can be used in case of small problems or problems, which are not sparse. All solvers use a Sequential Quadratic Programming (SQP) or Interior Point (IP) code to find the solution of the NLP problems. For very small problems also global optimisation methods, like the classical genetic algorithm CGA, can be used.

The use of gradient optimisation methods involves various requirements on all models used for the calculation of the trajectory and any other discipline. The model shall be differentiable and continuous, fast in computational time and the model computation shall depend only on a single call with a defined parameter calling, but not on internal state integration or similar approaches.

### 3. ASTOS FOR CDO

As mentioned previously, four disciplines have been included in the design optimisation: trajectory, aerodynamics, thermodynamics and weights.

The design optimisation is based on ASTOS' trajectory optimisation approach. Vehicle discipline analysis is performed at each point on the trajectory to assess the quality of the vehicle and the trajectory. The optimiser can then vary discipline parameters at the same time in one large parametric optimisation problem. The disciplines are interconnected either by direct exchange of data within the software code or by constraints.

To increase computational efficiency, the aerodynamics discipline has been split into shape parameterisation and aerodynamic computation of these shapes.

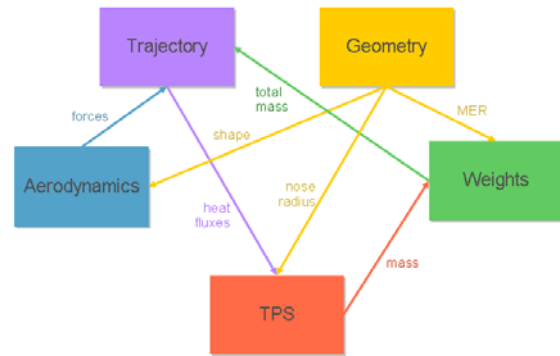


Figure 1 -Data exchange between disciplines

#### 3.1. Trajectory

The trajectory computation is considered to be the central part of the CDO software. The approach is that each discipline computes its state at any time point during the trajectory computation. The advantage is that trajectory and vehicle are optimisable under full consideration of various path and boundary constraints and cost functions. ASTOS allows the definition of more than 120 different constraints and more than 20 different cost functions. Some constraints, which are of particular interest for vehicle design optimisation, are: maximum normal and axial acceleration limit, maximum dynamic pressure limit, maximum heat flux and integrated heat flux, ground station visibility.

Typical cost functions for re-entry vehicles are: minimum loads (heat flux, dynamic pressure, g-load...), maximum robustness, to fulfil scientific mission aspects in the best way, (e.g. maximum time with certain heat flux). ASTOS allows the definition of multiple cost functions which are combined by a scaling factor. Additionally, each subsystem model can define its own constraints, cost functions, optimisable parameters and controls and derivatives for integration.

#### 3.2. Geometry

Five basic parameterised re-entry vehicle shapes are defined in the geometry module: four as proposed in [2] (sphere-cone, bi-conic, capsule and probe) and one as used in [3] (ellipsled).

##### Sphere-cone

The simplest shape is a sphere cone with no back shell. It is parameterized with only three parameters: the cone angle, the cone base radius and the nose radius (Fig. **Figure 2**).

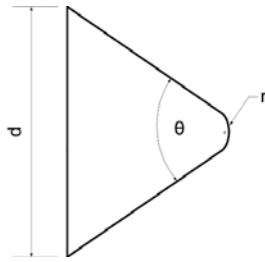


Figure 2 - Sphere cone shape, with parameters

### Capsule

The capsule shape is a simple shape with four parameters that define its fore body which is a calotte and its frustum back shell (Figure 3). It can be used for Apollo-like re-entry vehicles.

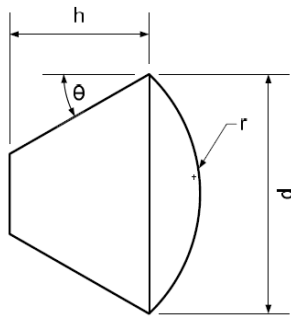


Figure 3 - Capsule shape, with parameters

### Probe

The probe shape is another simple shape with four parameters that define its sphere-cone fore-body and its back shell that is a calotte. It may be used for re-entry vehicles similar to e.g. Stardust.

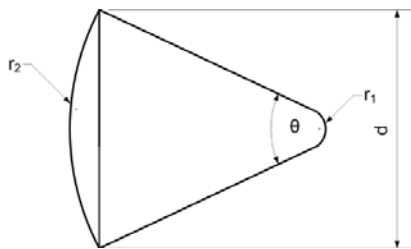


Figure 4 - Probe shape, with parameters

### Bi-conic

The bi-conic shape is essentially built with two cones, so that for the fore body there are five parameters: two cone angles, two cone base diameters and the nose radius. The back shell is composed of two frustums, which are parameterised by their cone angles and the height (Fig. Figure 5).

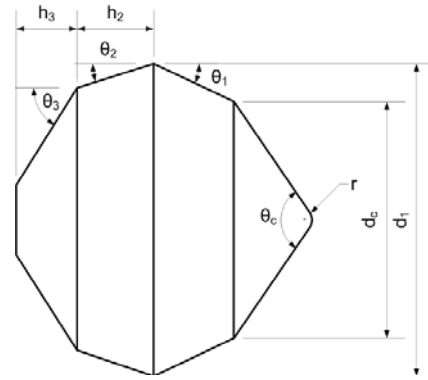


Figure 5 - Bi-conic shape, with parameters

### Ellipsled

The ellipsled shape is composed of two quarter-ellipsoids and a back shell whose section is accordingly composed of two half-ellipses. It is the only basic shape that is not rotationally symmetric. It needs five parameters as can be seen in Fig. Figure 6.

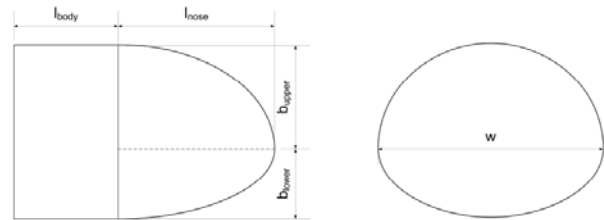


Figure 6 - Ellipsled shape, with parameters

### 3.3. Aerodynamics

The aerodynamics module calculates the aerodynamic properties of the vehicle as is configured by the geometry module for the whole flight regime, bounded by a Mach number range, an angle of attack range, and a yaw angle range. For this purpose the aerodynamic code SOSE – a surface inclination method developed by DLR – [16] has been integrated into ASTOS. SOSE can be used above a velocity of  $M=2.5$ .

Parting from a geometry indicated by the geometry module it can calculate aerodynamic coefficients ( $C_L$ ,  $C_D$ ,  $C_Q$ ,  $C_l$ ,  $C_m$ ,  $C_n$  and  $A_{wet}$ ), and the surface flow variables of the vehicle (pressure coefficient, free stream pressure ratio and Mach number as a function of the location along the vehicle).

Vehicle geometry is represented by a surface grid consisting out of arbitrary blocks, creating flat plates (panels) along the surface. Each flat plate possesses a characteristic normal-to-the-surface direction that allows SOSE to calculate the inclination. The pressure distribution along the surface of the vehicle is calculated based on the local surface inclination of the plates. All shapes present in the geometry module can be calculated with SOSE.

The aerodynamic properties are calculated for an inviscid flow, according to classical hypersonic theory as described in [4].

In order to add the effects of viscid flow the following correction can be added to the drag:

$$C_{D_{tot}} = C_D + C_{Df} \quad (1)$$

$$C_{Df} = C_f A_{wetted} / A_{ref}$$

Where  $C_D$  is the drag coefficient found by SOSE,  $C_{Df}$  is the skin friction drag coefficient;  $C_f$  is the turbulent skin friction coefficient,  $A_{wetted}$  the wetted surface and  $A_{ref}$  the reference area.

The location of the centre of pressure can be calculated for an angle of attack through the relation of the normal force coefficient to the moment coefficient at the leading edge [5]:

$$x_{cp} = \frac{C_m}{C_N} l \quad (2)$$

where  $C_m$  and  $C_N$  are calculated within SOSE. From the centre of pressure and the centre of gravity locations the static stability condition can be verified [6]:

$$x_{cg} - x_{cp} < 0 \quad (3)$$

### 3.4. Thermodynamics and TPS

The Thermal Protection System (TPS) is a critical part of a re-entry vehicle. It protects the vehicle structure and its interior from the heat load generated by aero heating, which is especially severe during hypersonic flight.

The objective is to design a TPS with minimum mass and with reliable performance. Therefore the analysis of the TPS needs to output the following two things:

- estimate of TPS weight
- TPS maximum temperatures

The weight is needed for the computation of the total vehicle mass which is used by the trajectory analysis. The TPS maximum temperatures are necessary to make sure that the TPS material will not fail during re-entry because of temperatures higher than the material allowable temperatures. The TPS is usually built up of more than one layer where each layer has different thermal properties.

The one-dimensional transient heat conduction within the TPS material is described by the energy balance equation at the TPS surface and the in-depth heat conduction equation for all layers:

$$q_{conv} + \alpha q_{rad} - \varepsilon \sigma T_{surf}^4 - q_{cond} = 0 \quad (4)$$

$$\frac{\partial}{\partial x} \left( \lambda_j \frac{\partial T}{\partial x} \right) - \rho_j c_{p,j} \frac{\partial T}{\partial t} = 0 \quad (5)$$

where  $T$  is the temperature,  $\lambda_j$  the thermal conductivity of layer  $j$ ,  $x$  the coordinate starting at the TPS surface,  $\rho_j$  the material density at layer  $j$ ,  $c_{p,j}$  the material's specific heat at layer  $j$ ,  $q_{conv}$  the convective heat flux,  $q_{rad}$  the radiative heat flux,  $q_{cond}$  the conductive heat flux,  $\varepsilon$  the material emissivity,  $\alpha$  the material absorptivity and  $\rho$  the Stephan/Boltzmann constant.

At the layer bounds the heat conduction equations for

each layer are connected by the following condition that essentially equals the outgoing heat flux of layer  $j$  and the incoming heat flux of layer  $j+1$ :

$$-\lambda_j \frac{\partial T}{\partial x} = -\lambda_{j+1} \frac{\partial T}{\partial x} \quad (6)$$

This implies that there is a perfect thermal contact between both layers.

The convective heat flux can be approximated following [7] (see also [8]):

$$q_{conv} = \frac{11.03 \cdot 10^7}{\sqrt{r_{nose}}} \sqrt{\frac{\rho_\infty}{\rho_{SL}}} \left( \frac{v_\infty}{v_{CO}} \right)^{3.0} \quad (7)$$

where  $r_{nose}$  is the nose radius,  $\rho_\infty$  the free stream air density,  $\rho_{SL}$  the air density at sea level,  $v_\infty$  the free stream velocity and  $v_{CO}$  the circular orbit velocity. The radiative heat flux from the gas into the TPS is, according to [3]:

$$q_{rad} = 7.9 \cdot 10^{11} r_{nose} \left( \frac{\rho_\infty}{\rho_{SL}} \right)^{1.5} \left( \frac{v_\infty}{10^4} \right)^{12.5} \quad (8)$$

This formula is valid for flight speeds:  $v_\infty \geq 6000$  m/s. Radiation from the gas into the TPS becomes relevant especially for high-speed re-entries. For example during the Apollo re-entry the radiative heat transfer accounted for more than 30% of the total heating [4].

#### Ablation

In case of ablation there are two effects that change the thermal response of the material. The first one is the one aimed at that some of the heat entering the TPS is carried away with the ablating material. More precisely, there is pyrolysis gas energy absorption, pyrolysis gas convection through the solid and surface chemistry. The second effect is the negative side effect that the material will decompose during ablation. Thereby the material density will decrease. The first effect can only be simulated with a complex model where the surface recession will be accounted for by changing the 1D thermal response grid.

Usually the backward nodes of the grid are deleted with ongoing surface recession and the whole TPS material is virtually shifted towards the surface. This approach was considered too complex within this study and was therefore not used. Rather, the approach shown in [9] was followed where the material decomposition is accounted for whereas the heat flux reduction due to ablation is neglected. This approach is conservative but of course less precise as it will over-predict the peak heat fluxes.

The material decomposition is computed explicitly as if it was a material property [9]. For the change in density the Arrhenius equation is used:

$$\frac{\partial \rho}{\partial t} = -A \left( \frac{E}{RT} \right) \rho_v \left( \frac{\rho - \rho_v}{\rho_v} \right)^\eta \quad (9)$$

where A is the pre-exponential factor, E the activation energy, R the universal gas constant,  $\rho_v$  the density of the virgin material,  $\rho_c$  the density of the charred material and  $\eta$  the density exponent factor. The surface recession rate can be computed using the heat of ablation [10] and assuming steady-state ablation (which is a conservative assumption):

$$\dot{s} = \frac{q_{hw}}{\rho Q^*} \quad (10)$$

where  $q_{hw}$  is the hot wall heat flux and  $Q^*$  the heat of ablation. The surface recession rate can then be integrated in order to get the total surface recession.

#### Discretisation

The in-depth heat (Eq.4) is a partial differential equation (PDE). It can be transformed into a set of ordinary differential equations (ODE) by the Method of Lines (see [11] for a general introduction and [12] for detailed examples on how to implement the method). This set of ODEs may then be integrated with a general-purpose ODE integrator like the ones that are used in ASTOS. The ODEs are discretised in all but one variable, which is the time in the case of Eq. 2.

The conductive heat flux within the material in Equation (8-2) according to Fourier's first law is:

$$q_{cond} = -\lambda \frac{\partial T}{\partial x} \quad (11)$$

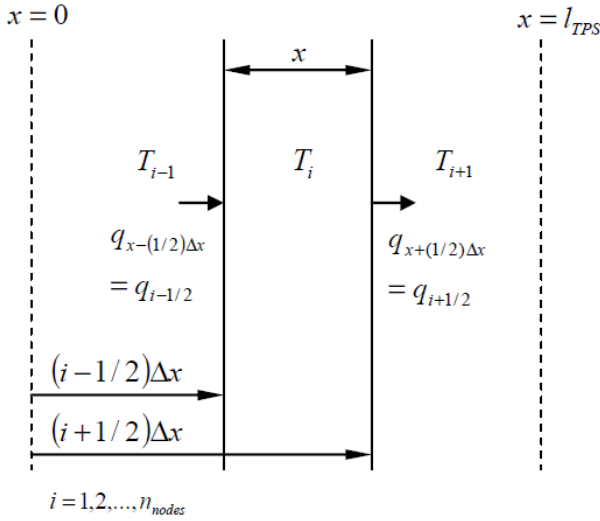


Figure 7 - Discretisation of the heat conduction equation

For the derivation of the ODEs describing this equation the spatial discretisation used is shown in Figure 7, following [12]. We compute the energy balance for one spatially discretised incremental volume of the TPS. The accumulation of heat is equal to the incoming heat flux minus the outgoing heat flux, so that:

$$\Delta x \rho c_p \frac{dT_i}{dt} = q_{i-1/2} - q_{i+1/2} \quad (12)$$

Combining this with Fourier's first law and after some rewriting the time derivative of the temperature at node I can be expressed as:

$$\frac{dT_i}{dt} = \frac{\lambda}{\rho c_p} \left( \frac{T_{i+1} - 2T_i + T_{i-1}}{\Delta x^2} \right) \quad (13)$$

The approach shown leads to an explicit integration of the nodal temperatures.

The initial and boundary conditions for Eq.12 are:

$$\begin{aligned} T(x, t = 0) &= T_0 \\ -k \frac{\partial T(x, t = 0)}{\partial x} &= q_{conv} + \alpha q_{rad} - \varepsilon \sigma T(x = 0, t)^4 \quad (14) \\ \frac{\partial T(x = l_{TPS}, t)}{\partial x} &= 0 \end{aligned}$$

where the middle condition is the energy balance for the TPS surface as described by Eq. 3. It prescribes the heat flux into the surface. The third equation assumes adiabatic conditions at the TPS back face. This is a conservative assumption as it assumes that the vehicle interior can not store any heat.

#### TPS sizing

TPS sizing is done according to the All-At-Once approach described in [1]. The optimal TPS thickness will be chosen by the optimizer along with the trajectory optimisation. Therefore the TPS thickness is an optimisable parameter within the entire optimisation problem. This is in contrast to common approaches like the one by [9] where the optimal TPS thickness is chosen separately from the optimal trajectory in an iterative way.

#### 3.5. Weights

The mass of a re-entry vehicle is mainly composed of its structural mass and the mass of the TPS system. The structural mass may be estimated with the following equation:

$$m_{structural} = aA + b \quad (15)$$

where A is the vehicle surface area and a and b are coefficients that have to be chosen appropriately. With the TPS thickness and the area to be covered with TPS the mass is calculated as:

$$m_{TPS} = \frac{Q_{ave}}{Q_{max}} \sum_{j=1}^{n_{layers}} V_j \rho_j = \frac{Q_{ave}}{Q_{max}} \sum_{j=1}^{n_{layers}} A_{TPS} t_j \rho_j \quad (16)$$

where  $\rho_j$  is the density and  $t_j$  is the thickness of the j-th TPS layer.  $Q_{ave}/Q_{max}$  is the ratio between the average heat load with respect to the streamline location and the maximum heat load. This approach is a simplification but can be justified as shown in the publication of [14].

If no specific TPS properties have been assigned to the capsule, the TPS mass is estimated with the following

formula [15]:

$$m_{TPS} = 0.091m_0Q^{0.51575} \quad (17)$$

where  $m_0$  is the vehicle total mass and  $Q$  is the total heat load encountered during re-entry.

#### 4. ACKNOWLEDGEMENT

The activities summarised in this paper have been performed by Astos Solutions under contract with ESA/ESTEC. The aerodynamics code SOSE has been integrated with the help of Thino Eggers of the DLR Institute of Aerodynamics and Flow Technology.

#### 5. REFERENCES

1. Tedford, N. P., Martins, J. R. R. A.,(2006) On the common structure of MDO problems: A comparison of architectures, Proceedings of the 11th AIAA/ISSMO Multidisciplinary Analysis and Optimization Conference, AIAA 2006-7080.
2. D.M. Kipp, J.A. Dec, G.W. Wells, R.D. Braun (2005). Development of a Planetary Entry System Synthesis Tool for Conceptual Design and Analysis, Proceedings of the 3rd International Planetary Probe Workshop.
3. J. Theisinger, R.D. Braun (2007). Hypersonic Entry Aeroshell Shape Optimisation, Master Thesis, Georgia Institute of Technology.
4. J. Anderson (1989). Hypersonic and High Temperature Gas Dynamics, McGraw-Hill.
5. J.D. Anderson (2001). Fundamentals of Aerodynamics, McGraw-Hill.
6. J.A.Mulder (2000). Flight Dynamics reader for the AE3-302 course, TU Delft.
7. R. W. Detra, H. Hidalgo, Generalized Heat Transfer Formulas and Graphs for Nose-Cone Re-Entry Into the Atmosphere, ARS Journal, March 1961, pp. 318 - 321
8. E. H. Hirschel (2005). Basics of Aerothermodynamics, Progress in Astronautics and Aeronautics, Springer-Verlag.
9. J.A. Dec, R. D. Braun (2006). An Approximate Ablative Thermal Protection System Sizing Tool for Entry System Design, AIAA 2006-780.
10. W. L. Hankey (1988). Re-Entry Aerodynamics, AIAA.
11. W. E. Schiesser(1991). The Numerical Method of Lines, Academic Press.
12. H.J. Lee, W. E. Schiesser (2003). Ordinary and Partial Differential Equation Routines in C, C++, Fortran, Java, Maple, and MATLAB, Chapman & Hall.
13. C. Gogu, T. Matsumura, R. T. Haftka, A. V. Rao, (2009). Aeroassisted Orbital Transfer Trajectory Optimization Considering Thermal Protection System Mass, Journal of Guidance, Control and Dynamics, Vol. 32, No. 3, pp. 927-938.
15. B. Laub (2003). Ablative Thermal Protection: An Overview, NASA Ames Research Centre.
16. Weihs, Hendrik and Turner, John and Longo, Jose Maria (2008) The Sharp Edge Flight Experiment SHEFEX II, a Mission Overview and Status. AIAA International Space Planes and Hypersonic Systems nad Technologies Conference , 2008-04-28 - 2008-05-01 , Dayton, OH (USA)